Interaction of OH Radicals with Arizona Test Dust: Uptake and Products

ARTICLE *in* THE JOURNAL OF PHYSICAL CHEMISTRY A · DECEMBER 2012

Impact Factor: 2.69 · DOI: 10.1021/jp311235h · Source: PubMed

3 AUTHORS:

Yuri Bedjanian
CNRS Orleans Campus
67 PUBLICATIONS **853** CITATIONS
SEE PROFILE

Manolis N Romanias
Ecole des Mines de Douai
25 PUBLICATIONS **99** CITATIONS
SEE PROFILE

Atallah El Zein
Université du Littoral Côte d'Opale (ULCO)
13 PUBLICATIONS **119** CITATIONS
SEE PROFILE

THE JOURNAL OF PHYSICAL CHEMISTRY A

Article

pubs.acs.org/JPCA

Interaction of OH Radicals with Arizona Test Dust: Uptake and Products

Yuri Bedjanian,* Manolis N. Romanias, and Atallah El Zein

Institut de Combustion, Aérothermique, Réactivité et Environnement (ICARE), CNRS, 45071 Orléans Cedex 2, France

ABSTRACT: Kinetics and products of the interaction of OH radicals with solid films of Arizona Test Dust (ATD) were studied using a low pressure flow reactor (0.5−3 Torr) combined with a modulated molecular beam mass spectrometer for monitoring of the gaseous species involved. The reactive uptake coefficient of OH was measured from the kinetics of OH consumption on Pyrex rods coated with ATD as a function of OH concentration ($(0.4-5.2) \times 10^{12}$ molecules cm^{-3}), relative humidity (RH = 0.03−25.9%), temperature (T = 275−320 K), and UV irradiance intensity (J_{NO_2} = 0−0.012 s^{-1}). Deactivation of ATD surface upon exposure to OH was observed. The initial uptake coefficient was found to be independent of temperature and irradiation conditions and to decrease with relative humidity: $\gamma_0 = 0.2/(1 + RH^{0.36})$ (calculated using geometric surface area, with 30% estimated conservative uncertainty). H_2O_2 and H_2O were observed in the gas phase as products of the OH reaction with ATD surface with yields of (10 ± 3) and (98 ± 25) %, respectively.

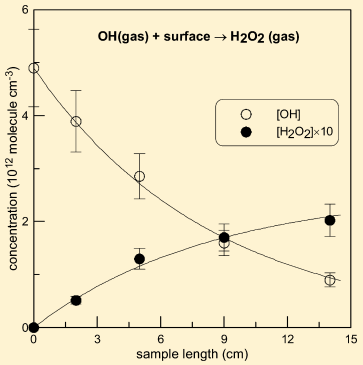

1. INTRODUCTION

The OH radical is the main atmospheric oxidant responsible for the degradation of most natural and anthropogenic trace gases.[1] This radical is known to have a short atmospheric lifetime determined by its loss processes in the gas phase. Therefore, it is clear that even a very efficient heterogeneous loss of OH on atmospheric aerosol (up to the maximum uptake probability of unity) will be negligible compared to the gas phase loss and will not impact the OH concentration in the atmosphere. However, heterogeneous reactions of OH are recognized to be important in processing of atmospheric aerosol leading to modification of its chemical composition as well as of its physical properties.[2] For instance, hydroxyl radical may take part in photodegradation of particulate organic matter.[2−7] In these processes the OH radical uptake is often the rate-limiting step for the entire process of physicochemical transformation of aerosol particles.[4] In this respect, the kinetic and mechanistic information on the interaction of OH radicals with solid substrates of atmospheric relevance seems to be of interest for laboratory studies on oxidative aging of aerosols especially with submonolayer organic coating.

The information on OH uptake available in literature is rather limited especially when compared with that for other atmospheric oxidants.[8] The information on the products and mechanism of the OH interaction with the surfaces of atmospheric interest is practically absent. The aim of the current study was to investigate the interaction of OH with Arizona Test Dust (ATD) surface under dark and UV irradiation conditions as a function of relative humidity and temperature. Arizona Test Dust is a mixture of metal oxides, which are generally present in atmospheric mineral aerosol in various proportions. The choice of ATD in this study was motivated by a desire to mimic (at least, to some extent) the chemical composition of atmospheric particles. According to recent estimations, every year 1600 Tg of mineral dust is released in the atmosphere.[9] Although the primary sources of the dust particles are arid regions, due to the global air circulation aerosol particles undergo long-range transport to populated areas and influence the air quality and public health.[10,11] The dust surfaces provide the seedbed for trace gas molecules adsorption-reaction and therefore are considered to play a key role in the transformation and environmental fate of many atmospheric species.[12,13]

2. EXPERIMENTAL SECTION

2.1. Preparation of Mineral Samples. Solid films of ATD were deposited on the outer surface of a Pyrex tube (0.9 cm o.d.) using a suspension of ATD (Powder Technology Inc., nominal 0−3 μm ATD) in ethanol. Prior to film deposition, the Pyrex tube was treated with hydrofluoric acid and washed with distilled water and ethanol. Then, the tube was immersed into the suspension, withdrawn, and dried with a fan heater. As a result, rather homogeneous (to eye) solid films were formed at the Pyrex surface. In order to eliminate the possible residual traces of ethanol, prior to uptake experiments, the freshly prepared ATD samples were heated at (100 − 150)°C during (20 − 30) min under pumping. In order to measure the mass of the sample on the Pyrex tube, the deposited solid film was mechanically removed at the end of the kinetic experiments. BET surface area of the ATD powder was determined using a Quantachrome-Autosorb-1-MP-6 apparatus and nitrogen as adsorbate gas and was found to be 85 ± 10 m^2 g^{-1}.

Received: September 18, 2012
Revised: December 17, 2012
Published: December 18, 2012

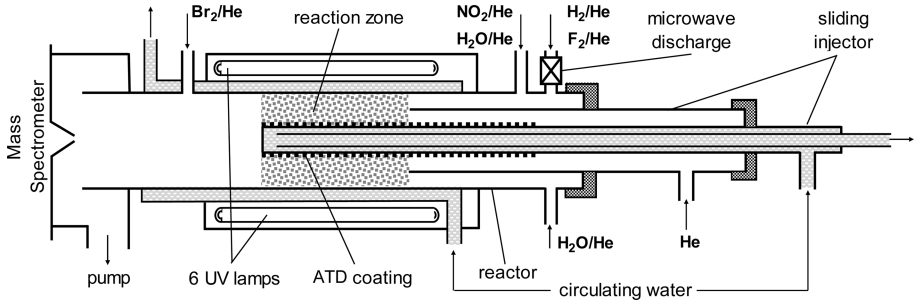

Figure 1. Diagram of the flow reactor.

2.2. Flow Reactor. Interaction of OH with solid ATD films was studied at 1−3.2 Torr total pressure of He (used as a carrier gas) in a discharge flow reactor with mass spectrometric detection of the gaseous species involved. The experimental equipment and approach used for the kinetic measurements were described in previous papers from this group.[7,14−16] The main reactor (Figure 1) consisted of a Pyrex tube (40 cm length and 2.4 cm i.d.) with a jacket for the thermostatted liquid circulation. Experiments were carried out using a coaxial configuration of the flow reactor with movable triple central injector: the Pyrex tube with deposited sample was introduced into the main reactor along its axis. The coated tube could be moved relative to the outer tube of the injector that allowed the variation of the solid film length exposed to gas phase reactant and consequently of the reaction time defined by the sample length/flow velocity ratio. The linear flow velocity in the reactor was in the range 2800−3100 cm s^{-1} in all the experiments except a few ones in the measurements of RH dependence (Table 1). The third (inner) tube of the movable injector was used for circulation of the thermostatted liquid inside the tube covered with solid sample. This allowed to maintain the same temperature in the main reactor and on the ATD sample surface in the measurements of the temperature dependence of the uptake coefficient. In addition, the ATD sample could be heated by means of a coaxial cylindrical heater introduced inside the coated tube.

The walls of the main reactor as well as of the outer tube of the movable injector (in contact with OH) were coated with halocarbon wax in order to minimize the heterogeneous loss of OH outside the reaction zone.

Externally, the reactor was surrounded by 6 UV lamps (Sylvania BL350, 8 W) with a broad UV emission spectrum between 315−400 nm. The UV lamps were installed into an aluminum light-tight box covering the main reactor tube. Therefore, by switching on or off the lamps, we had the ability to perform kinetic measurements under UV irradiation or dark conditions, respectively. The irradiance intensity in the reactor was characterized by direct measurements of the NO_2 photolysis frequency, J_{NO_2}, as a function of the number of lamps switched on. The values of J_{NO_2} determined in a direct way from kinetics of NO_2 loss in the presence of UV irradiation in the flow tube were found to be between 0.002 and 0.012 s^{-1} for 1 to 6 lamps switched on, respectively.[16]

2.3. Generation of OH Radicals and Measurement of Absolute Concentrations. Two different methods were used for the generation of OH radicals. In the first one, the fast reaction of hydrogen atoms with NO_2 was used as a source of OH radicals, H atoms being produced in a microwave discharge of H_2/He mixture:

$$H + NO_2 \rightarrow OH + NO \quad (1)$$

NO_2 was always used in excess over H atoms. In the second method, OH radicals were produced in the reaction of F atoms with an excess of H_2O, with F atoms formed in the microwave discharge of the F_2/He mixture:

$$F + H_2O \rightarrow OH + HF \quad (2)$$

It was verified by mass spectrometry that more than 90% of F_2 was dissociated in the microwave discharge. To reduce F atom reactions with the glass surface inside the microwave cavity, a ceramic (Al_2O_3) tube was inserted in this part of the discharge tube. Water vapor was introduced into the flow reactor by passing He through thermostatted glass bubbler with deionized water.

OH radicals were detected as $HOBr^+$ (m/z = 96/98) after scavenging by an excess of Br_2 (added downstream of the reaction zone) via reaction:

$$OH + Br_2 \rightarrow Br + HOBr \quad (3)$$

This method of OH detection was preferred to the direct detection of these radicals at m/z = 17 (OH^+) because of significant contribution of water vapor at this mass. All other

Table 1. Dependence of the Initial Uptake Coefficient of OH to ATD Surface on Relative Humidity: Experimental Conditions and Results (T = 275 K, $[OH]_0 \approx 10^{12}$ molecules cm^{-3})

RH (%)	P (Torr)	flow velocity (cm s^{-1})	k' (s^{-1})	$k'_{corrected}$ (s^{-1})	γ_0	source of OH
3.5×10^{-4}	0.5	2823	1146	1736	0.163	H + NO_2
1.7×10^{-2}	0.5	2828	1083	1596	0.150	H + NO_2
2.3×10^{-2}	0.5	3121	1037	1498	0.141	H + NO_2
3.5×10^{-2}	0.5	2833	1115	1667	0.157	H + NO_2
5.5×10^{-2}	0.5	3091	1029	1390	0.125	F + H_2O
0.10	0.5	2851	923	1274	0.120	F + H_2O
0.34	0.5	2925	933	1300	0.122	H + NO_2
0.52	0.5	2984	907	1255	0.118	F + H_2O
0.56	0.5	2875	893	1248	0.117	H + NO_2
2.9	0.5	3218	616	799	0.075	H + NO_2
3.3	0.6	3082	594	770	0.072	F + H_2O
6.5	0.7	3192	476	635	0.060	H + NO_2
7.3	0.8	3136	435	581	0.055	H + NO_2
10.6	1.0	3160	428	645	0.061	F + H_2O
13.7	1.5	1842	341	553	0.052	H + NO_2
25.9	3.3	927	193	359	0.037	H + NO_2

dx.doi.org/10.1021/jp311235h | J. Phys. Chem. A 2013, 117, 393−400

species (Br_2, NO_2, H_2O, and H_2O_2) were detected at their parent peaks.

The same procedure of OH chemical conversion to HOBr by an excess of Br_2 was used for the measurements of the absolute concentrations of the radicals: [OH] = [HOBr] = $\Delta[Br_2]$. Thus, OH concentrations were determined from the consumed fraction of Br_2. The possible influence of secondary chemistry on the applied procedure of the OH detection and absolute concentration measurements was discussed previously and was shown to be negligible.[17,18] The initial concentration of OH radicals in the kinetic study of their uptake on ATD surface was in the range (0.4−5.2) × 10^{12} molecules cm^{-3}. Concentrations of the stable species, Br_2 and NO_2, were determined from the pressure drop in flasks of known volume containing Br_2/He and NO_2/He mixtures of known dilution. The absolute calibration of H_2O_2 has been performed by injecting known amounts (0.5−10 μL) of the 60 wt % solution inside the flow tube reactor and recording the parent mass peak intensity of H_2O_2 at m/z = 34. The integrated area of the mass spectrometric signals corresponding to the known total number of H_2O_2 molecules injected into the reactor allowed the determination of the calibration factor. The concentrations of water vapor were determined by calculating the H_2O flow rate from the total (H_2O + He) and H_2O vapor pressures in the bubbler and the measured flow rate of He through the bubbler.

3. RESULTS AND DISCUSSION

3.1. Kinetics of OH Loss. Figure 2 displays a typical behavior of the concentration of OH radicals upon introduction

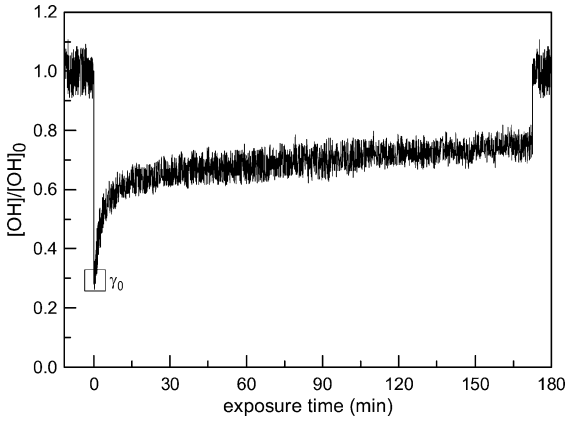

Figure 2. Typical uptake profiles of OH on ATD surface: T = 300 K, P = 0.5 Torr, dry conditions, $[OH]_0 \approx 10^{12}$ molecules cm^{-3}, sample mass = 0.2 mg cm^{-1} × 3 cm.

of the ATD coated tube into the reaction zone (t = 0). Fast initial consumption of OH, followed by surface deactivation resulting in a decrease of OH loss rate, was observed. When the mineral sample was withdrawn from the reaction zone after exposure to OH ($t \approx$ 170 min), that is when OH was no longer in contact with the sample surface, the concentration of OH recovered rapidly to its initial value. Considering that steady-state uptake is never achieved and the reactive surface cannot be defined at long reaction times (see section 3.3), only the initial uptake coefficient of OH (γ_0) (and not the steady-state one) was measured in the present work.

The uptake coefficient was determined as the probability of irreversible loss of the radicals per collision with dust surface

$$\gamma = \frac{4k'}{\omega}\frac{V}{S} \quad \text{(I)}$$

where k' is the first order rate coefficient of OH loss (s^{-1}), ω the average molecular speed (cm s^{-1}), V the volume of the reaction zone (cm^3), and S the surface area of the solid sample involved in the heterogeneous reaction (cm^2).

Figure 3 (open circles) displays an example of OH loss kinetics in heterogeneous reaction with the surface of ATD

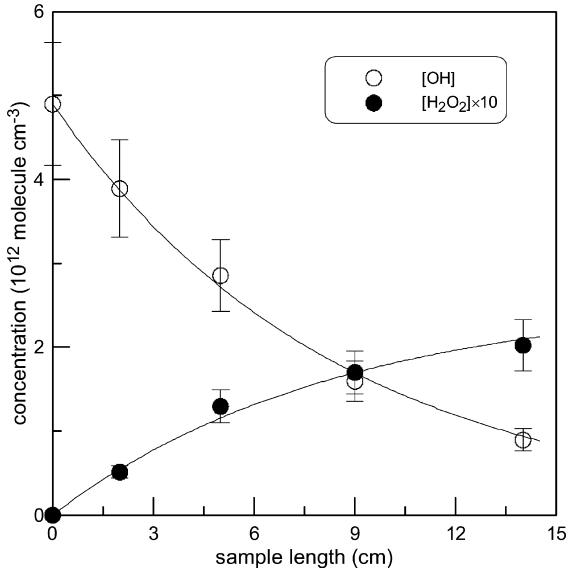

Figure 3. Example of kinetics of OH consumption and product, H_2O_2, formation in the heterogeneous reaction of OH with ATD surface: T = 300 K, P = 0.5 Torr, dry conditions, ATD sample mass = 0.7 mg cm^{-1}.

(under quasi steady-state uptake conditions). These data were obtained by varying the length of mineral film in contact with OH, which is equivalent to varying the reaction time. The decays of OH were found to be exponential (solid line in Figure 3) and were treated with the first-order kinetics formalism, the rate constant being determined as

$$k'_{obs} = -\frac{d\ln([OH])}{dt} \quad \text{(II)}$$

where t is the reaction time defined by the sample length to flow velocity ratio. The values of the observed first-order rate constants, k'_{obs}, determined from the decays of OH should be corrected for the diffusion limitation in the OH radial transport from the volume to the reactive surface. The radial diffusion problem for the coaxial configuration of the reactor used in the present study was solved by Gershenzon and co-workers:[19,20]

$$\frac{1}{k'_{obs}} = \frac{1}{k'} + \frac{R^2}{K^d(q)D_0} \times P \quad \text{(III)}$$

where k' is the true rate constant, D_0 is the diffusion coefficient of OH at 1 Torr pressure (Torr cm^2 s^{-1}), P is the total pressure in the reactor, and $K^d(q)$ is a dimensionless rate constant of radial diffusion, which is a function of sample tube radius (r) to main reactor radius (R) ratio, $q = r/R$ = 0.375 (for configuration used in the present study). Diffusion corrections on k'_{obs} were calculated using expression III with $D_0 = 640 \times (T/298)^{1.85}$ Torr cm^2 s^{-1},[7,21,22] and $K^d(q)$ = 4.4.[19] In order to reduce rather elevated diffusion corrections on k'_{obs} due to high uptake of OH to ADT surface, experiments were carried out at

dx.doi.org/10.1021/jp311235h | J. Phys. Chem. A 2013, 117, 393−400

the relatively low pressure of 0.5 Torr (except a few runs for RH dependence where higher pressure was used). Ultimately, the diffusion corrections applied to k'_{obs} were generally between 30 and 50%; however, for a few points measured at elevated pressures (up to 3 Torr), they reached a factor as high as 1.8 (see Table 1).

3.2. Dependence on Sample Mass. In this series of experiments, the uptake of OH was measured as a function of the thickness of ATD sample exposed to OH. The objective was to determine the surface area of the solid film involved in the interaction with OH radicals. The experiments were performed at T = 300 K under dry conditions. The obtained results are presented in Figure 4, where the uptake coefficient

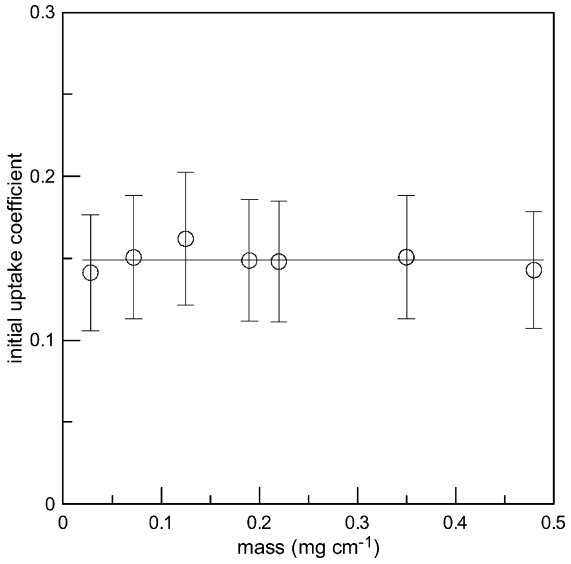

Figure 4. Dependence of the initial uptake coefficient of OH (calculated using the geometric surface area) on mass of ATD samples (per 1 cm length of the support tube): T = 300 K, P = 0.5 Torr, dry conditions, $[OH]_0 \approx 10^{12}$ molecules cm^{-3}.

of OH, calculated applying the geometric (projected) surface area of ATD sample, is shown as a function of the ATD mass deposited per unity length of the support tube. The results of these experiments show that the OH loss probability does not depend on the mass of mineral sample (i.e., on the thickness of coating). This indicates that, under the experimental conditions used, only the outer surface (or uppermost part) but not the entire surface area of the solid film interacts with OH. This probe depth involved in the heterogeneous reaction cannot be determined in the present experiments. Consequently, we use the geometric surface area of the ATD samples for the calculations of the uptake coefficient. Considering that the measured values of γ_0 are very high and, consequently, the OH penetration depth into the powder sample is expected to be very limited, this approximation seems to be reasonable. Nevertheless, the value of γ_0 from the present study should be considered as an upper limit for the uptake coefficient.

3.3. Dependence on Initial Concentration of OH. The dependence of γ_0 on initial concentration of OH radicals, varied in the range (0.4−5.2) × 10^{12} molecules cm^{-3}, was measured at T = 300 K under dry conditions. The observed results are shown in Table 2. The uptake coefficient was found to decrease with increasing $[OH]_0$: γ_0 falls down by a factor about 2.5 upon increase of $[OH]_0$ by nearly 1 order of magnitude. Generally,

Table 2. Dependence of the Uptake Coefficient of OH to ATD Surface on Initial Concentration of OH (Dry Conditions, T = 300 K, P = 0.5 Torr, Sample Mass = (0.3−0.4) mg cm^{-1})

$[OH]_0$ (10^{12} molecules cm^{-3})	k' (s^{-1})	$k'_{corrected}$ (s^{-1})	γ_0
0.4	1380	2117	0.190
1.1	1178	1676	0.151
1.2	1072	1469	0.132
2.7	911	1183	0.106
5.2	684	827	0.074

initial uptake is not expected to be dependent on the gas phase concentration of the reactant since at the initial stage of the surface exposure, the active sites on the surface are not depleted or blocked and are all available for the heterogeneous reaction. Here, the observed decrease of the measured γ_0 with increasing initial concentration of OH is most likely due to very rapid uptake of OH radicals and rather small surface area (the geometric one) involved in the heterogeneous interaction, which results in the deactivation of the surface within the first seconds of the sample exposure to OH. In these circumstances, the limited time resolution of our detecting system would lead to a "cutting" of the sharp peak corresponding to initial OH adsorption. The deactivation of the surface may be due to its progressive saturation with the products of heterogeneous reaction, H_2O being the most probable final reaction product remaining on the surface. Indeed, the calculations performed with the data presented in Figure 2 show that the integrated number of OH molecules taken up by the surface (geometric) within the first minute of exposure is already nearly 5 × 10^{16} molecules cm^{-2}, that is roughly by 2 orders of magnitude higher than monolayer coverage. This observation seems to clearly indicate that OH loss on ATD has a catalytic nature, i.e., is not limited by site-filling.

The measured OH dependent uptake coefficient is not a stand alone physical parameter but a complex function of a number of chemical and physical processes on the surface. In order to estimate the true initial uptake (accommodation coefficient), we extrapolated our data set to lower concentrations of OH. Figure 5 shows the dependence of the reciprocal of the measured uptake coefficient on initial concentration of OH. Intercept of the straight line provides the extrapolated value for the initial uptake coefficient of OH to ATD:

$$\gamma_0 = 0.20 \pm 0.02$$

where uncertainty is the 2σ statistical one. This value is close to that measured with the lowest concentration of OH, 4 × 10^{11} molecules cm^{-3}, in the present study (Table 2 and Figure 5) and can be considered as a reasonable approximation for lower concentrations of OH. Recall that the upper limit of γ_0 is 1.

The observed OH loss on ATD surface is nonreversible and partly catalytic. These features make difficult the parametrization of the time dependence of the uptake coefficient. Prolonged exposure to the compounds coming from OH sources used in the study (NO_2, H_2O_2, and HF) can also lead to modification of the surface reactivity with time, although no impact of these species on the initial uptake was observed (see below). Additional complexity in describing the temporal behavior of γ is associated with the definition of the dust surface involved in the heterogeneous interaction. The point is that, whereas the calculation of the initial uptake coefficient using

dx.doi.org/10.1021/jp311235h | J. Phys. Chem. A 2013, 117, 393−400

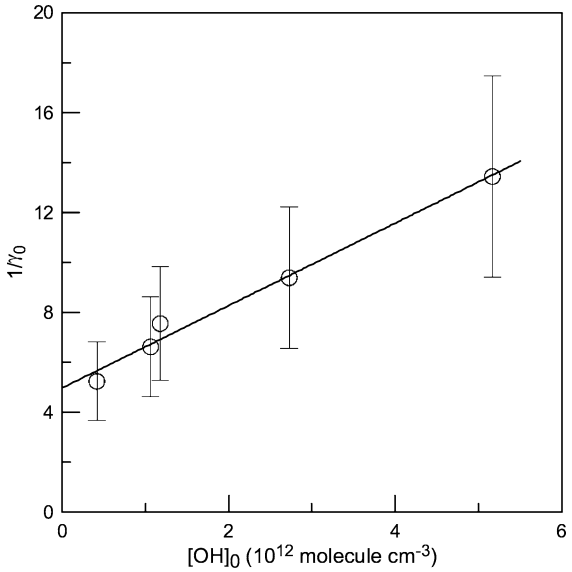

Figure 5. Reciprocal of the initial uptake coefficient of OH to ATD surface as a function of the initial OH concentration: T = 300 K, P = 0.5 Torr, sample mass = (0.3−0.4) mg cm^{-1}.

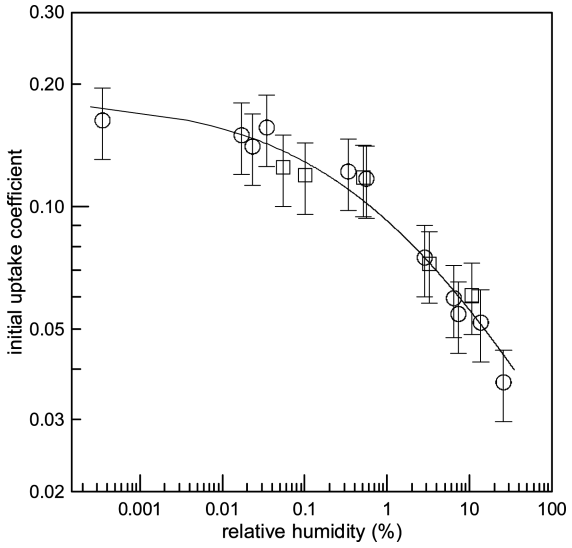

Figure 6. Initial uptake coefficient of OH on ATD as a function of relative humidity: T = 275 K, P = 0.5−3.2 Torr, $[OH]_0 \approx 10^{12}$ molecules cm^{-3}, sample mass = (0.4−0.5) mg cm^{-1}. The data were obtained with two sources of OH radicals: reactions H + NO_2 (circles) and F + H_2O (squares).

geometric surface area seems to be reasonable, the uptake at longer times can be influenced by transport into underlying dust layers. In fact, the time dependence of the measured uptake coefficient was found to be reasonably well described with a sum of two exponential functions, corresponding to rapid initial decrease of γ followed by its slower decline at longer exposure times. The diffusion into the bulk of, most probably, the stable reaction products (H_2O and H_2O_2) and not OH, leading to partial liberation of the active sites on the outer surface of the dust sample, could be a reasonable explanation for this reduction of the decrease rate of the uptake coefficient.

3.4. Dependence on RH, Temperature, and UV Irradiation Intensity. RH dependence of the uptake coefficient was studied at T = 275 K, with relative humidity in the reactor being varied in the range (3.5× 10^{-4}−25.9) %. Rather low temperature was chosen for these experiments in order to provide reasonably high RH in the reactor under relatively low total pressures used. Prior to uptake experiments (contact with OH), the freshly prepared and heated under pumping (as noted in the experimental section) samples of ATD were exposed during nearly 5 min to water vapor present in the reactor. The results obtained for initial uptake coefficient of OH on ATD surface are displayed in Table 1 and Figure 6. One can note that the uptake data obtained using different chemical systems for generation of OH radicals (circles and squares in Figure 6) are in agreement within the experimental uncertainty on the determination of γ_0 (estimated to be nearly 25%). This observation seems to indicate that the presence of NO_2 (when H + NO_2 reaction is used for generation of OH radicals) in the reactive system has a negligible impact on the uptake of OH radicals to ATD surface. This was verified in additional experiments where the uptake coefficient of OH was measured with concentration of NO_2 varied between 1 × 10^{13} and 1.4 × 10^{14} molecules cm^{-3}. The values of γ_0 measured in the presence of different concentrations of NO_2 in the reactor were found to be similar within 10% statistical uncertainty.

As it can be seen in Figure 6, the values of the uptake coefficient can be considered as RH independent under dry conditions (up to RH = 0.03%). However, significant decrease of γ_0 is observed when RH is further increased. The solid line in Figure 6 represents a power fit to the experimental data according to the following expression:

$$\gamma_0 = 0.18/(1 + RH^{0.36})$$

This is an empirical equation that allows describing our results in the whole RH range used with estimated conservative uncertainty of 30%.

Temperature dependence of the uptake coefficient was measured in the temperature range (275−320) K at a fixed relative humidity of 0.03%. The results are presented in Figure 7. As one can note, uptake coefficients were found to be independent of temperature.

Dependence of the uptake coefficient on the irradiation intensity was studied in additional experiments by switching on the different number of lamps in the reactor, from 1 to 6. This corresponds to the variation of the NO_2 photolysis frequency from 0.002 to 0.012 s^{-1}. Under these irradiance conditions, we have not observed any effect of the UV irradiation on the kinetics of OH loss on the ATD samples in the whole range of RH used. The measured values of γ_0 were similar (within a few %) to those under dark conditions.

3.5. Reaction Products. H_2O_2 and H_2O were observed to be released into the gas phase upon interaction of OH radicals with ATD surface. It should be noted that the formation of H_2O_2 observed in reaction of OH with fresh samples of ATD was somewhat delayed with respect to the OH consumption: $[H_2O_2]_{formed}$ to $[OH]_{consumed}$ ratio was found to increase during the first minutes of ATD exposure to OH and to become stable after nearly 15−20 min of exposure. For this reason, all the measurements presented below were conducted under steady-state uptake conditions where H_2O_2 yield was independent of the exposure time.

An example of the kinetics of OH consumption and concurrent formation of H_2O_2 observed in OH interaction with ATD surface is shown in Figure 3. Experimental data for

dx.doi.org/10.1021/jp311235h | J. Phys. Chem. A 2013, 117, 393−400

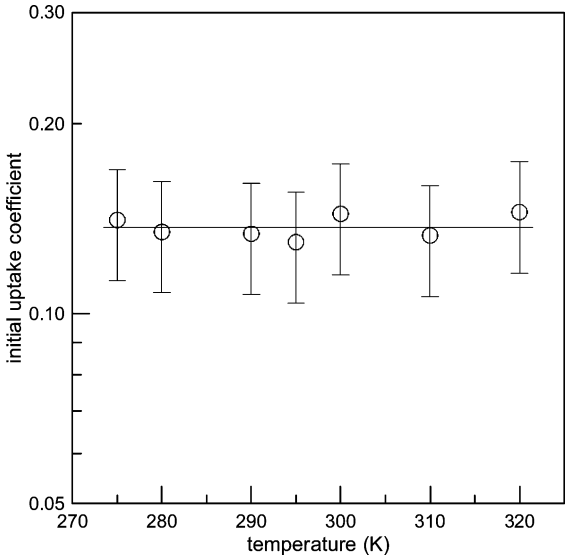

Figure 7. Temperature dependence of the uptake coefficient of OH on ATD: P = 0.5 Torr, T = 275–320 K, RH = 0.03%, $[OH]_0 \approx 10^{12}$ molecules cm^{-3}, sample mass = (0.4–0.5) mg cm^{-1}.

H_2O_2 are fitted (solid line) with an exponential function according to the following equation

$$[H_2O_2] = \alpha[OH]_0(1 - \exp(-k't))$$

where k' is the first order rate constant determined from the kinetics of OH consumption, and α is the branching ratio for the H_2O_2 forming reaction channel. The solid line corresponding to data for $[H_2O_2]$ in Figure 3 was obtained with the value of α = 0.053.

Figure 8 displays the concentrations of H_2O_2 and H_2O formed in the reaction of OH with ATD surface as a function of the consumed concentration of OH. These results were obtained with initial concentration of OH varied in the range 4.0×10^{11}–5.0×10^{12} and 1.9×10^{11}–2.6×10^{12} molecules cm^{-3} for monitoring of H_2O_2 and H_2O, respectively. One can note that the impact of the initial concentration of OH on the yield of both products was negligible. The straight lines in Figure 8 go through the origin and have the slopes of 0.050 ± 0.004 (2σ) and 0.49 ± 0.03 (2σ) corresponding to the ratio of the concentration of product (H_2O_2 and H_2O, respectively) formed to the concentration of OH consumed. These values result in nearly 10% and 98% yields for H_2O_2 and H_2O, respectively, if one considers the hydrogen mass balance (two OH radicals are lost to form one H_2O_2 or H_2O molecule).

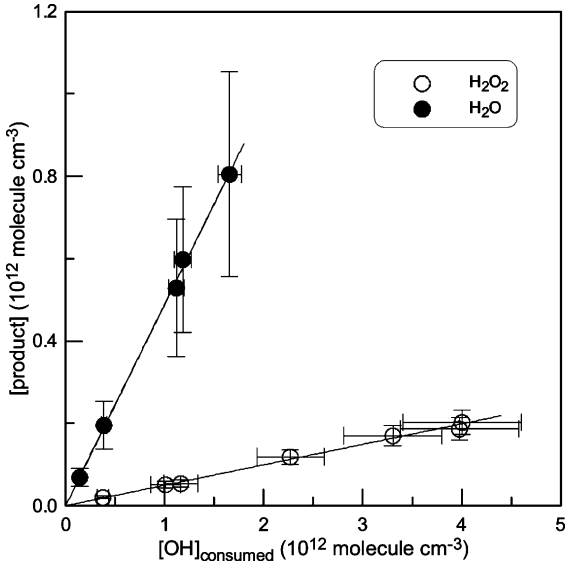

Figure 8. Concentrations of H_2O_2 and H_2O formed in the gas phase as a function of OH concentration lost on the surface of ATD sample: T = 300 K, P = 0.5 Torr, dry conditions, $[OH]_0$ = (0.4–5.0) × 10^{12} molecules cm^{-3}, sample mass = 0.7 mg cm^{-1}.

The possible impact of the secondary gas phase chemistry on the measured yield of the products can be briefly discussed. First, the data presented in Figure 3 clearly show that the observed H_2O_2 is a product of the heterogeneous reaction: concentration of H_2O_2 follows heterogeneous decay of OH and increases with the length of the mineral sample exposed to OH. In addition, the gas phase trimolecular recombination reaction of OH radicals[23]

$$OH + OH + M \rightarrow H_2O_2 + M$$
$$k_4 = 6.9 \times 10^{-31} \text{ cm}^6 \text{ molecule}^{-2} \text{ s}^{-1} \quad (4)$$

is too slow under experimental conditions of the present study to influence the measured concentrations of H_2O_2. From another side, H_2O_2 formed in the heterogeneous reaction can be consumed in secondary reaction with OH:[23]

$$OH + H_2O_2 \rightarrow HO_2 + H_2O$$
$$k_5 = 1.8 \times 10^{-12} \text{ cm}^3 \text{ molecule}^{-1} \text{ s}^{-1} \text{ (gas phase)} \quad (5)$$

Concerning possible impact of this reaction on H_2O_2 concentration in the gas phase, it is estimated to be below 10% for the maximum residence time in the reactor and maximum OH concentration of nearly 10^{-2} s and 5×10^{12} molecules cm^{-3}, respectively. The observed independence of the H_2O_2 yield of the initial concentration of OH also points to the negligible impact of the reaction 5 in the gas phase.

3.6. Comparison with Previous Data. This work reports the first measurement of the OH radical uptake to Arizona Test Dust. However, the results can be compared with the existing data on OH uptake to SiO_2 (silica) and Al_2O_3 (alumina), which are major components of mineral dust aerosol and ATD, in particular. Concerning the existing data on OH uptake to silica, one can note very large differences in reaction probabilities measured in different studies. The values reported for the uptake coefficient of OH under dry conditions ranged from $(2–6) \times 10^{-3}$[24,25] up to 0.4–0.6.[26,27] For comparison, the value of γ_0 measured in the present study on ATD surface under dry conditions is 0.20 ± 0.06 (estimated uncertainty of 30%). Suh et al.[25] suggested that the variations in the surface of SiO_2 are the cause of the differences in γ from the different studies. The data from the present study indicate that other experimental parameters such as time scale of experiments (surface deactivation, and decrease of γ with exposure time) and initial concentration of OH radicals can significantly impact the measurements of the uptake coefficient. Regarding the OH uptake data on Al_2O_3, the situation is similar to that for SiO_2, the reported values of γ being widely scattered: 0.005,[25] 0.04,[24] and 0.22.[21] In a recent study of Park et al.,[28] the values of $\gamma = (3.2 \pm 0.7) \times 10^{-2}$ and $(4.5 \pm 0.5) \times 10^{-2}$ under dry conditions were reported for SiO_2 and Al_2O_3, respectively. The values of γ measured by these authors under high humidity conditions (with RH up to 38%) had shown that water vapor enhanced

dx.doi.org/10.1021/jp311235h | J. Phys. Chem. A 2013, 117, 393–400

the OH uptake coefficient for both mineral oxides: the observed enhancement in γ for silica and alumina were a factor of 3 and 2, respectively, within an RH range of 0−38%. In order to explain the observed increase in the OH uptake rate under high humidity conditions, Park et al.[28] speculated that the presence of water leads to additional formation of functional OH groups on mineral surfaces, which facilitates their reactions with adsorbed or gas-phase OH via self-reaction under high humidity conditions. The RH dependence of γ observed in the present study (decrease of the uptake coefficient upon increase of RH) points to the role of water rather as blocking the available active sites on the surface and seems to be in line, at least qualitatively, with the available data for the adsorption of water on mineral oxides.[29,30] Indeed, it was reported that water adsorption to SiO_2, Al_2O_3, MgO, Fe_2O_3, and TiO_2 (which are components of ATD) could be well described with the Brunauer−Emmett−Teller (BET) type isotherm, with the monolayer coverage occurring between 20 and 30% relative humidity.[29,30] It can be noted that, in previous studies, similar negative dependence on RH was observed also for the uptake coefficient of H_2O_2 on SiO_2, Al_2O_3,[31] and TiO_2.[32,33]

3.7. Reaction Mechanism. Hydrogen peroxide and water have been observed as products of the interaction of OH radical with mineral surface. The observation of H_2O confirms the potential mechanisms discussed by Suh et al.[25] and Park et al.[28] assuming that the uptake of OH radicals is due to their adsorption to the surface followed by the reactions with another adsorbed or gas-phase OH. The reaction products, H_2O_2 and H_2O, can result from OH attack on preexisting surface OH groups and/or on OH adsorbed from the gas phase:

$$\{S\} + OH \rightarrow \{S{-}OH\} \quad (6)$$

$$\{S{-}OH\} + OH \rightarrow \{S\} + \{H_2O_2\} \quad (7)$$

$$\{S{-}OH\} + OH \rightarrow \{S{-}O\} + \{H_2O\} \quad (8)$$

where species in brackets denote reactants or products on the surface and S is a surface site. $\{S{-}O\}$ can be expected to react with OH forming surface bound HO_2 radical:

$$\{S{-}O\} + OH \rightarrow \{S{-}O{-}OH\} \quad (9)$$

The most probable fate of the surface HO_2 is its reaction with OH leading to the regeneration of the surface active site:

$$\{S{-}O{-}OH\} + OH \rightarrow \{S\} + \{H_2O\} + \{O_2\} \quad (10)$$

This simplified hypothetical mechanism is in line with the experimental observation of the reaction products, H_2O_2 and H_2O, in the gas phase upon their evaporation from the surface.

The yield of H_2O_2 was found to be independent of the initial concentration of OH radical. This seems to indicate that the rate of $\{S{-}OH\}$ processing via reactions 7 and 8 is higher than the rate of reaction 6. If so, the concentration of surface OH ($\{S{-}OH\}$) is in a steady-state, independent of OH concentration in the gas phase. Consequently, the rate of H_2O_2 forming reaction 7 is first order in [OH].

Unfortunately, the present data on yields of H_2O_2 and H_2O in the gas phase do not allow determining the distribution of the primary products of the surface reaction because of the possible chemical transformation of H_2O_2 on mineral surface. Indeed, preliminary data on the interaction of H_2O_2 with the surface of ATD (subject of our current investigation) show that the uptake of H_2O_2 to ATD is rather rapid and reactive, i.e., practically irreversible: $\gamma_0 \approx 0.001$ under dry conditions, decreasing upon surface exposure to a steady-state value which is by more than 1 order of magnitude lower. It is worth noting that the rapid initial uptake of H_2O_2 to ATD surface can be responsible for the observed delayed production of H_2O_2 with respect to OH consumption (see above). Products of the H_2O_2 interaction with ATD are not known but are expected to be O_2 and H_2O. In addition, in the presence of OH in the reactive system, reaction 11 can also contribute to the loss of surface H_2O_2 (similar to the gas phase):

$$\{H_2O_2\} + OH \rightarrow \{HO_2\} + \{H_2O\} \quad (11)$$

Finally, the above considerations show that water formed on the surface upon uptake of OH may result from primary and various secondary reactions and, in particular, from the transformation of primary reaction product H_2O_2. In this respect, the yields determined for H_2O_2 and H_2O should be considered as lower and upper limits, respectively.

The sequence of reactions 6−10 corresponds to a catalytic mechanism of the OH loss since surface active sites $\{S\}$ are not consumed provided that the reaction products are desorbed and do not block the active sites. Observed decrease of the uptake coefficient with exposure time indicates that final products of the heterogeneous reaction (most probably, H_2O) accumulate on the surface, leading to its progressive passivation. At first sight, accumulation of H_2O on the surface may seem to contradict the experimental observation of nearly 100% hydrogen mass balance between OH consumed on the surface and products in the gas phase. In this respect, it can be noted that, considering a very high number of OH radicals taken up by the surface (section 3.3), even a few percent of H_2O formed upon OH loss and not released into the gas phase will be enough to provide adequate surface coverage.

In conclusion, it can be noted that, although the title reaction has a limited atmospheric impact, the kinetic and, especially, mechanistic information from the present study seems to be very useful for laboratory studies dealing with OH processing of coated (with organics, for example) and uncoated surfaces of atmospheric relevance.

AUTHOR INFORMATION

Corresponding Author

*Tel: +33 238255474. Fax: +33 238696004. E-mail: yuri.bedjanian@cnrs-orleans.fr.

Notes

The authors declare no competing financial interest.

ACKNOWLEDGMENTS

This study was supported by ANR from Photodust grant. A.E.Z. is very grateful to Région Centre for financing his Ph.D. grant.

REFERENCES

(1) Finlayson-Pitts, B. J.; Pitts, J. N. J. *Chemistry of the Upper and Lower Atmosphere: Theory, Experiments and Applications*; Academic Press: San Diego, CA, 2000.

(2) George, I. J.; Vlasenko, A.; Slowik, J. G.; Broekhuizen, K.; Abbatt, J. P. D. *Atmos. Chem. Phys.* **2007**, *7*, 4187−4201.

(3) Ellison, G. B.; Tuck, A. F.; Vaida, V. *J. Geophys. Res.* **1999**, *104*, 11633−11641.

(4) Molina, M. J.; Ivanov, A. V.; Trakhtenberg, S.; Molina, L. T. *Geophys. Res. Lett.* **2004**, *31*, L22104.

(5) Esteve, W.; Budzinski, H.; Villenave, E. *Atmos. Environ.* **2006**, *40*, 201−211.
(6) McNeill, V. F.; Yatavelli, R. L. N.; Stipe, C. B.; Landgrebe, O. *Atmos. Chem. Phys.* **2008**, *8*, 5465−5476.
(7) Bedjanian, Y.; Nguyen, M. L.; Le Bras, G. *Atmos. Environ.* **2010**, *44*, 1754−1760.
(8) Crowley, J. N.; Ammann, M.; Cox, R. A.; Hynes, R. G.; Jenkin, M. E.; Mellouki, A.; Rossi, M. J.; Troe, J.; Wallington, T. J. *Atmos. Chem. Phys.* **2010**, *10*, 9059−9253.
(9) Andreae, M. O.; Rosenfeld, D. *Earth Sci. Rev.* **2008**, *89*, 13−41.
(10) Kanatani, K. T.; Ito, I.; Al-Delaimy, W. K.; Adachi, Y.; Mathews, W. C.; Ramsdell, J. W. *Am. J. Respir. Crit. Care Med.* **2010**, *182*, 1475−1481.
(11) Usher, C. R.; Michel, A. E.; Grassian, V. H. *Chem. Rev.* **2003**, *103*, 4883−4940.
(12) Dentener, F. J.; Carmichael, G. R.; Zhang, Y.; Lelieveld, J.; Crutzen, P. J. *J. Geophys. Res.* **1996**, *101*, 22869−22889.
(13) Kolb, C. E.; Cox, R. A.; Abbatt, J. P. D.; Ammann, M.; Davis, E. J.; Donaldson, D. J.; Garrett, B. C.; George, C.; Griffiths, P. T.; Hanson, D. R.; et al. *Atmos. Chem. Phys.* **2010**, *10*, 10561−10605.
(14) Bedjanian, Y.; Lelièvre, S.; Le Bras, G. *Phys. Chem. Chem. Phys.* **2005**, *7*, 334−341.
(15) Loukhovitskaya, E.; Bedjanian, Y.; Morozov, I.; Le Bras, G. *Phys. Chem. Chem. Phys.* **2009**, *11*, 7896−7905.
(16) El Zein, A.; Bedjanian, Y. *Atmos. Chem. Phys.* **2012**, *12*, 1013−1020.
(17) Bedjanian, Y.; Le Bras, G.; Poulet, G. *J. Phys. Chem. A* **1999**, *103*, 7017−7025.
(18) Bedjanian, Y.; Le Bras, G.; Poulet, G. *Int. J. Chem. Kinet.* **1999**, *31*, 698−704.
(19) Gershenzon, Y. M.; Grigorieva, V. M.; Ivanov, A. V.; Remorov, R. G. *Faraday Discuss.* **1995**, *100*, 83−100.
(20) Gershenzon, Y. M.; Grigorieva, V. M.; Zasypkin, A. Y.; Remorov, R. G. Theory of radial diffusion and first order wall reaction in movable and immovable media. In *Proceedings of the 13th International Symposium on Gas Kinetics*, Dublin, Ireland, 1994; pp 420−422.
(21) Bertram, A. K.; Ivanov, A. V.; Hunter, M.; Molina, L. T.; Molina, M. J. *J. Phys. Chem. A* **2001**, *105*, 9415−9421.
(22) Ivanov, A. V.; Trakhtenberg, S.; Bertram, A. K.; Gershenzon, Y. M.; Molina, M. J. *J. Phys. Chem. A* **2007**, *111*, 1632−1637.
(23) Sander, S. P.; Abbatt, J.; Barker, J. R.; Burkholder, J. B.; Friedl, R. R.; Golden, D. M.; Huie, R. E.; Kolb, C. E.; Kurylo, M. J.; Moortgat, G. K.; et al. *Chemical Kinetics and Photochemical Data for Use in Atmospheric Studies, Evaluation No. 17*; JPL Publication 10-6; Jet Propulsion Laboratory: Pasadena, CA, 2011.
(24) Gershenzon, Y. M.; Ivanov, A. V.; Kucheryavyi, S. I.; Rozenshtein, V. B. *Kinet. Catal.* **1986**, *27*, 923−927.
(25) Suh, M.; Bagus, P. S.; Pak, S.; Rosynek, M. P.; Lunsford, J. H. *J. Phys. Chem. B* **2000**, *104*, 2736−2742.
(26) Bogart, K. H. A.; Cushing, J. P.; Fisher, E. R. *J. Phys. Chem. B* **1997**, *101*, 10016−10023.
(27) Fisher, E. R.; Ho, P.; Breiland, W. G.; Buss, R. J. *J. Phys. Chem.* **1993**, *97*, 10287−10294.
(28) Park, J.-H.; Ivanov, A. V.; Molina, M. J. *J. Phys. Chem. A* **2008**, *112*, 6968−6977.
(29) Goodman, A. L.; Bernard, E. T.; Grassian, V. H. *J. Phys. Chem. A* **2001**, *105*, 6443−6457.
(30) Ma, Q.; He, H.; Liu, Y. *J. Environ. Sci.* **2010**, *22*, 555−560.
(31) Zhao, Y.; Chen, Z.; Shen, X.; Zhang, X. *Environ. Sci. Technol.* **2011**, *45*, 3317−3324.
(32) Pradhan, M.; Kalberer, M.; Griffiths, P. T.; Braban, C. F.; Pope, F. D.; Cox, R. A.; Lambert, R. M. *Environ. Sci. Technol.* **2010**, *44*, 1360−1365.
(33) Romanias, M. N.; El Zein, A.; Bedjanian, Y. *J. Phys. Chem. A* **2012**, *116*, 8191−8200.